JOC*Article*

Medium Effects on the Decarboxylation of a Biotin Model in Pure and Mixed Solvents from QM/MM Simulations

Orlando Acevedo and William L. Jorgensen*

Department of Chemistry, Yale University, 225 Prospect Street, New Haven, Connecticut 06520-8107.

william.jorgensen@yale.edu.

Received March 10, 2006

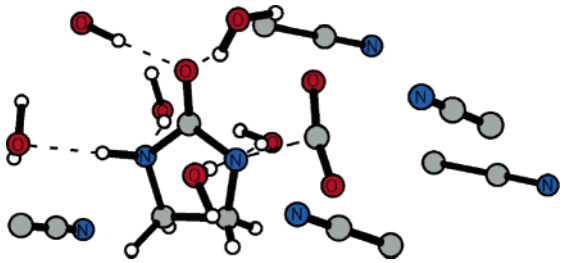

The decarboxylation of imidazolidin-2-one-1-carboxylate anion **2** has been investigated via combined quantum and statistical mechanics methodology. Monte Carlo statistical mechanics simulations utilizing free-energy perturbation theory and PDDG/PM3 for the QM method yielded free-energy profiles for the reaction in water, methanol, acetonitrile, and mixed solvents. The results for free energies of activation are uniformly in close accord with experimental data and reflect large rate accelerations in progressing from protic to dipolar aprotic media. Structural and energetic analyses confirm that the rate retardation in protic solvents comes from loss of hydrogen bonding in progressing from the carboxylate anion **2** to the more charge-delocalized transition state (TS). The structure of the TS is found to be significantly affected by the reaction medium; it occurs at a 0.2-Å shorter C−N separation in protic solvents than in acetonitrile. Characterization of the hydrogen bonding for **2** and the TS also provided insights for design of decarboxylase catalysts, namely, it is desirable to have three hydrogen-bond donating groups positioned to interact with the ureido oxygen along with two hydrogen-bond donors positioned to interact with the ureido nitrogen of the breaking C−N bond.

Introduction

Biotin plays a crucial role as an organic cofactor in the formation of malonyl-CoA, vital in the metabolism of fatty acids (Scheme 1).[1] Carboxyl transfer enzymes, acyl-CoA carboxylases (ACCase), utilize biotin as a ferry for the delivery of a carboxylate group between two unique active sites located within different domains of the enzyme. The active site in the biotin carboxylase domain is responsible for carboxylation at the N1 position of biotin,[2] while the active site in the carboxytransferase domain controls the elimination of CO_2.[3,4] *N*(1′)-carboxybiotin is known to be inherently unreactive and must be activated for the decarboxylation. Several mechanisms have been discussed for the enzymatic elimination step,[1,4−9] and many issues regarding the intrinsic reactivity of carboxybiotin also remain

SCHEME 1. Transfer of Carbon Dioxide from the Enzymatic Intermediate *N*(1′)-Carboxybiotin

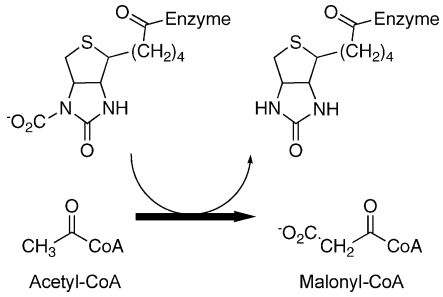

(1) (a) Knowles, J. R. *Annu. Rev. Biochem.* **1989**, *58*, 195−221. (b) Cronan, J. E., Jr.; Waldrop, G. L. *Prog. Lipid Res.* **2002**, *41*, 407−435.

(2) (a) Athappilly, F. K.; Hendrickson, W. A. *Structure* **1995**, *3*, 1407−1419. (b) Roberts, E. L.; Shu, N.; Howard, M. J.; Broadhurst, R. W.; Chapman-Smith, A.; Wallace, J. C.; Morris, T.; Cronan, J. E., Jr.; Perham, R. N. *Biochemistry* **1999**, *38*, 5045−5053.

(3) Zhang, H.; Tweel, B.; Li, J.; Tong, L. *Structure* **2004**, *12*, 1683−1691.

(4) Diacovich, L.; Mitchell, D. L.; Pham, H.; Gago, G.; Melgar, M. M.; Khosla, C.; Gramajo, H.; Tsai, S. C. *Biochemistry* **2004**, *43*, 14027−14036.

10.1021/jo060533b CCC: $33.50
Published on Web 05/28/2006

under investigation, specifically, protonation state, medium effects, metal-ion chelation, and geometrical distortion upon binding at the active site. As an important model, fundamental insights have been sought through kinetic studies for imidazolidin-2-one-1-carboxylic acid (**1**) and its carboxylate anion (**2**).[5,8,9] In particular, the rate of decarboxylation of **1** is notably sensitive to pH and choice of solvent.[6,9] In water, the rate decreases sharply with increasing pH until about pH 8 where it levels off, which is consistent with different elimination mechanisms for the protonated and ionized forms. The pK_a of **1** is 4.2, so in neutral aqueous solution it is predominantly ionized; the anion **2** has a half-life of 3.2 h at 25 °C. At high pH the reaction is much faster in dipolar aprotic solvents than protic ones with relative rates of 1, 49, and 517 for water, methanol, and acetonitrile.[9b,c] The slow rate at high pH is thought to reflect the relative instability of the product anion **3**, while the rate retardation in protic solvents stems from better hydrogen bonding with **2** than for the more charge-delocalized transition state (TS) leading to **3**.

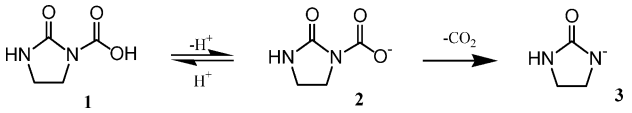

To gain further insights into the decarboxylation of the biotin model **2** in solution, the present combined quantum and statistical mechanics (QM/MM) study has been carried out. The approach features quantum mechanical treatment of the reacting system in the presence of hundreds of explicit solvent molecules with computation of free-energy profiles using free-energy perturbation (FEP) theory in Monte Carlo statistical mechanics (MC) simulations. Such studies permit detailed elucidation of the changes in solvation along the reaction paths and of the associated reaction-rate variations in different media. Insights into catalyst design can also emerge through elucidation of the optimal hydrogen-bonding patterns for the reactant and TS. Furthermore, prior to extending our computational investigations of the mechanisms of enzymatic reactions to decarboxylations,[10] it is important to validate and calibrate the methodology for the uncatalyzed processes. Good success was previously found in investigations of solvent and internal hydrogen-bonding effects on the rates of decarboxylation for 3-carboxybenzisoxazoles,[11] while attention is turned here to the biotin model **2**.

The most closely related prior computational study for the decarboxylation of **2** was reported by Gao and Pan in 1999.[12] At that time, the reaction was only studied in water; a series of gas-phase structures along the reaction path were optimized by ab initio calculations with subsequent QM(AM1)/MC/FEP calculations between these rigid structures to estimate the effect of hydration on the activation barrier.[12] In the present approach, the QM calculations for the reacting system are again performed during the MC/FEP calculations, and the solute is fully sampled. The present calculations have also been performed in water, methanol, and acetonitrile as well as mixed solvent systems to parallel fully the experimental study of Rahil et al.[9b,c] Importantly, the complete sampling of the geometry of the reacting system permits characterization of the changes in the geometries of reactants, TSs, and products in the different media.

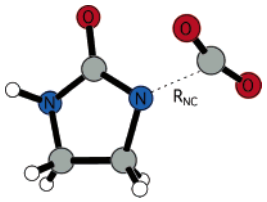

FIGURE 1. Reaction coordinate, R_{NC}, for the decarboxylation of **2**. Illustrated structure is the transition structure from gas-phase PDDG/PM3 calculations, R_{NC} = 2.39 Å.

Computational Methods

QM/MM calculations[13] were carried out using BOSS 4.6,[14] with the reacting system treated using the semiempirical PDDG/PM3 method.[15] PDDG/PM3 has been tested for gas-phase structures and energetics[15] and has performed well in solution-phase QM/MM studies of S_N2 reactions,[16] a nucleophilic aromatic substitution (S_NAr),[17] Kemp decarboxylations,[11] and Cope eliminations.[18] Nonaqueous solvent molecules are represented with the united-atom OPLS force field, and the TIP4P model is used for water.[19,20] The systems consisted of the reacting system plus 395 nonaqueous solvent molecules or 740 water molecules. The simulation cell is periodic and tetragonal with c/a = 1.5, where a is about 25, 27, and 29 Å for water, methanol, and acetonitrile.

FEP calculations were performed in conjunction with Metropolis MC simulations in the NPT ensemble at 25 °C and 1 atm. A free-energy profile was computed in each solvent to locate the minima and maxima along the reaction path. The solvent molecules only translate and rotate, while all internal degrees of freedom for the reacting system were sampled except for the reaction coordinate, R_{NC} in Figure 1. R_{NC} was perturbed from 1.40 to 5.40 Å, with an increment of 0.01 Å. In our recent QM/MM studies, ΔR increments of 0.01−0.02 Å have been typical to enhance precision for computed activation barriers.[11,16−18] Each FEP calculation entailed 2.5 million configurations of equilibration followed by 5 million configurations of averaging. Solute−solvent and solvent−solvent intermolecular cutoff distances of 12 Å were employed based on all heavy atoms of the solute, the oxygens of water and methanol, and

(5) (a) Caplow, M. *J. Am. Chem. Soc.* **1965**, *87*, 5774−5785. (b) Caplow, M.; Yager, M. *J. Am. Chem. Soc.* **1967**, *89*, 4513−4521.
(6) Thatcher, G. R. J.; Poirier, R.; Kluger, R. *J. Am. Chem. Soc.* **1986**, *108*, 2699−2704.
(7) Tipton, P. A.; Cleland, W. W. *J. Am. Chem. Soc.* **1988**, *110*, 5866−5869.
(8) Lihs, F. J.; Caudle, M. T. *J. Am. Chem. Soc.* **2002**, *124*, 11334−11341.
(9) (a) Kluger, R.; Tsao, B. *J. Am. Chem. Soc.* **1993**, *115*, 2089−2090. (b) Rahil, J.; You, S.; Kluger, R. *J. Am. Chem. Soc.* **1996**, *118*, 12495−12498. (c) Rahil, J.; You, S.; Kluger, R. *J. Am. Chem. Soc.* **1998**, *120*, 2692.
(10) For example, see: Guimarães, C. R. W.; Udier-Blagovic, M.; Jorgensen, W. L. *J. Am. Chem. Soc.* **2005**, *127*, 3577−3588.
(11) Acevedo, O.; Jorgensen, W. L. *J. Am. Chem. Soc.* **2005**, *127*, 8829−8834.
(12) Gao, D.; Pan, Y. K. *J. Org. Chem.* **1999**, *64*, 1151−1159.
(13) (a) Åqvist, J.; Warshel, A. *Chem. Rev.* **1993**, *93*, 2523−2544. (b) Gao, J. *Acc. Chem. Res.* **1996**, *29*, 298−305. (c) Kaminski, G. A.; Jorgensen, W. L. *J. Phys. Chem. B* **1998**, *102*, 1787−1796.
(14) Jorgensen, W. L.; Tirado-Rives, J. *J. Comput. Chem.* **2005**, *26*, 1689−1700.
(15) (a) Repasky, M. P.; Chandrasekhar, J.; Jorgensen, W. L. *J. Comput. Chem.* **2002**, *23*, 1601−1622. (b) Tubert-Brohman, I.; Guimarães, C. R. W.; Repasky, M. P.; Jorgensen, W. L. *J. Comput. Chem.* **2003**, *25*, 138−150. (c) Tubert-Brohman, I.; Guimarães, C. R. W.; Jorgensen, W. L. *J. Chem. Theory Comput.* **2005**, *1*, 817−823.
(16) Vayner, G.; Houk, K. N.; Jorgensen, W. L.; Brauman, J. I. *J. Am. Chem. Soc.* **2004**, *126*, 9054−9058.
(17) Acevedo, O.; Jorgensen, W. L. *Org. Lett.* **2004**, *6*, 2881−2884.
(18) Acevedo, O.; Jorgensen, W. L. *J. Am. Chem. Soc.* **2006**, *128*, 6141−6146.
(19) (a) Jorgensen, W. L. *J. Phys. Chem.* **1986**, *90*, 1276−1284. (b) Jorgensen, W. L.; Briggs, J. M. *Mol. Phys.* **1988**, *63*, 547−558.
(20) Jorgensen, W. L.; Chandrasekhar, J.; Madura, J. D.; Impey, W.; Klein, M. L. *J. Chem. Phys.* **1983**, *79*, 926−935.

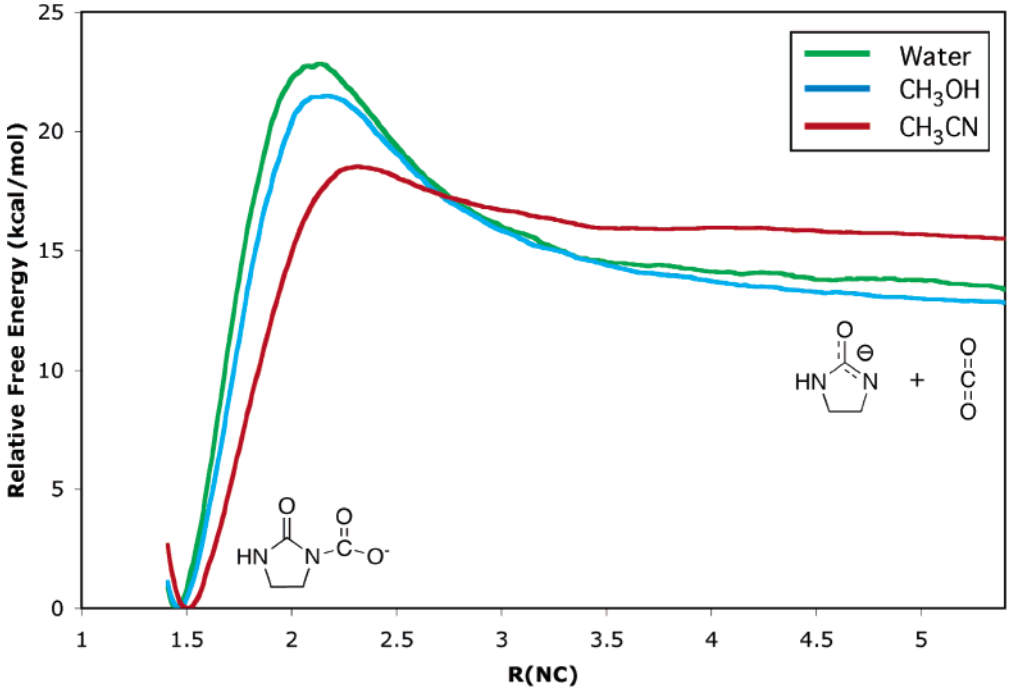

FIGURE 2. Computed free-energy profiles in water, methanol, and acetonitrile for the reaction of **2** at 25 °C.

TABLE 1. Computed R_{NC} Distances (Å) for 2 and the TS at 25 °C and 1 atm[a]

	water	CH_3OH	CH_3CN
reactant	1.45	1.47	1.51
TS	2.14	2.18	2.32

[a] Statistical uncertainties are ±0.02 Å.

TABLE 2. Free Energies of Activation and Reaction (kcal/mol) for the Decarboxylation of 2

	$\Delta G^{\ddagger}$ (calcd)[a]	$\Delta G^{\ddagger}$ (exptl)[b]	ΔG_{rxn} (calcd)[c]
water	22.8	23.2	13.4
CH_3OH	21.5	20.9	12.8
CH_3CN	18.5	19.5	15.5

[a] Statistical uncertainty is ±0.2 kcal/mol. [b] References 9b,c. [c] Statistical uncertainty is ±0.5 kcal/mol.

the central carbon of acetonitrile. If any distance is within the cutoff, the entire solute−solvent or solvent−solvent interaction was included. For electrostatic contributions to the solute−solvent energy, unscaled CM3 atomic charges[21] were obtained for the solute in conjunction with the PDDG/PM3 calculations for the solute's energy. Computation of the QM energy and atomic charges was performed for every attempted solute move, that is, every 100 configurations. If a MC configuration is accepted, then the QM energy, charges, and solute−solvent energies for the two perturbed solutes ($\Delta R_{NC} = \pm 0.01$ Å) are also computed for the application of the Zwanzig equation.[22] The number of single-point QM calculations required for one free-energy profile was about 15 million, clearly showing the need for a highly efficient QM method. A single FEP calculation for the aqueous system required about 1 h on a 3 GHz Pentium IV running Linux, and a full free-energy profile required about 8 days. The FEP calculations are automated so that an entire free-energy profile is obtained through one job submission.[14]

Results and Discussion

Energetics and Structure. The computed free-energy profiles for the reaction in pure water, methanol, and acetonitrile are shown in Figure 2. The geometrical and free-energy results are summarized in Tables 1 and 2. Immediately, it is apparent that there is an interesting geometrical effect with significantly shorter R_{NC} separations for both **2** and the TS in the protic solvents. In the extreme, as R_{NC} lengthens, the charged CO_2 fragment departs and becomes neutral. Thus, the shorter R_{NC} distances in the protic solvents are accompanied by more charge on the carboxylate group, which results in better solvation through hydrogen bonding. For **2**, PDDG/PM3 optimization in the gas-phase yields $R_{NC} = 1.52$ Å, which is close to the average value in acetonitrile; the shortening to 1.45 Å in water is accompanied by a 0.02 e increase in the negative charge on both carboxylate oxygens to about −0.66 e. For the TS, the same effect leads to a nearly 0.2 Å shortening of R_{NC} in going from acetonitrile to water. This is also interesting because, although the activation barrier is lower in acetonitrile, the TS occurs later. In comparison, the computed solvent effects on the breaking C−C bond were modest for the decarboxylation of 3-carboxybenzisoxazole;[11] however, the product anion (a phenoxide) is more stable in that case, and the TS occurs earlier near 2.0 Å.

The effect of solvent choice on the free-energy profiles is striking in the vicinity of the TSs (Figure 2). The expected pattern with significantly higher activation barriers in the protic solvents is quantitatively well reproduced; the experimental and FEP results for the free energies of activation, $\Delta G^{\ddagger}$, are in close accord (Table 2). This is especially significant in view of the complexity of the modeled system and the need for the correct description of the intramolecular energetics and solvation. It does continue the pattern of good results found for the decarboxylation of 3-carboxybenzisoxazoles.[11] It should also be noted that the present calculations did not include a counterion, so the accord between theory and experiment is consistent with a lack of ion pairing for **2** and the TS with K^+ as counterion under the experimental conditions.[9]

(21) Thompson, J. D.; Cramer, C. J.; Truhlar, D. G. *J. Comput. Chem.* **2003**, *24*, 1291−1304.
(22) Zwanzig, R. W. *J. Chem. Phys.* **1954**, *22*, 1420−1426.

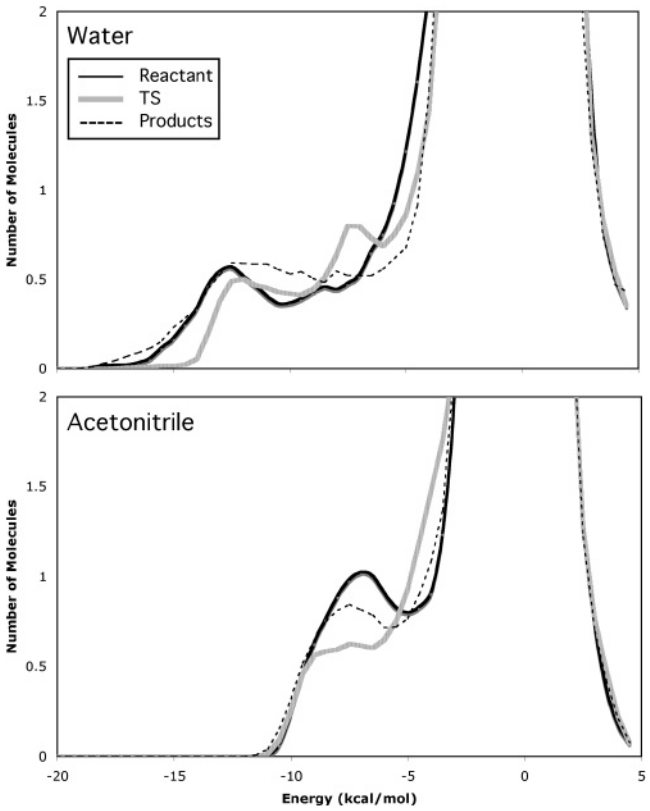

FIGURE 3. Solute−solvent energy pair distributions for the decarboxylation of **2** in water and acetonitrile for the reactant, the TS, and the products. The ordinate records the number of solvent molecules that interact with the solutes with their interaction energy on the abscissa. Units for the ordinate are number of molecules per kcal/mol.

On the technical side, notably smooth free-energy profiles (Figure 2) were obtained in view of the 0.01 Å increment for ΔR_{NC}. Therefore, the statistical uncertainties in the computed $\Delta G^{\ddagger}$ values are small. They have been estimated from the fluctuations in the ΔG values for each FEP window using the batch means procedure with batch sizes of 0.5 M configurations. The statistical uncertainties ($1\sigma_i$) were only 0.001−0.03 kcal/mol in each window; thus, the overall uncertainties in the computed $\Delta G^{\ddagger}$ values in Table 2 are about 0.2 kcal/mol (ca. $(0.02^2 \times 100 \text{ windows})^{1/2}$). The uncertainties for ΔG_{rxn} are about 0.5 kcal/mol.

Gao and Pan also obtained good accord between their calculated $\Delta G^{\ddagger}$ (22.7 ± 0.2 kcal/mol) and the experimental result in water.[12] However, the fact that solute sampling was not performed in their MC/FEP calculations may be related to their prediction of no shift in the position of the TS in water versus the gas phase (2.2 Å). In the present case, the PDDG/PM3 value for R_{NC} drops from 2.39 Å for gas-phase optimization (Figure 1) to 2.32, 2.18, and 2.14 Å from the QM/MM/FEP simulations in acetonitrile, methanol, and water. The latter results seem qualitatively reasonable, as discussed above, and allowance of full geometrical response for the reacting system is clearly desirable in simulations of condensed-phase reactions.

Solvation. Detailed insights on the changes in solvation along the reaction pathways are available from the present QM/MM/MC calculations. Specifically, the solute−solvent energy pair distributions record the average number of solvent molecules that interact with the solute and the associated energy. The results for the decarboxylation of **2** in water and acetonitrile are shown in Figure 3; results for methanol can be found in the Supporting Information. Hydrogen bonding in water and the most favorable ion−dipole interactions in acetonitrile are reflected in the left-most region, with solute−solvent interaction energies more attractive than about −5 kcal/mol. The large bands near 0 kcal/mol result from the many distant solvent molecules in outer shells.

In water, strong hydrogen bonds are apparent for the reactant and product anions, with interaction energies in the −10 to −20 kcal/mol range; integration of the curves yields 4.4 and 5.3 such interactions for the reactant and products. Owing to the charge delocalization in the TS, there are fewer interactions in this range (3.1) and they are weaker on average by about 2 kcal/mol. In acetonitrile, the strongest solute−solvent interactions are only about −10 kcal/mol, and the differences between reactant, TS, and products are diminished. Integration to −5 kcal/mol yields about 9, 7, and 8 interactions, respectively, and the corresponding numbers in water are 10, 9, and 11. This description is consistent with the display of instantaneous configurations, for example, for **2** and the TS in water in Figure 4. There are eight hydrogen-bonded water molecules in both snapshots, but the hydrogen-bond lengths are shorter for **2**, particularly for the carboxylate oxygens. For the TS, the shortest hydrogen bonds are for the ureido N and O that are formally receiving the negative charge. The overall picture supports the fact that hydrogen bonding is very sensitive to charge distributions, so it is more affected by the progression from **2** to the TS than the weaker ion−dipole interactions in a dipolar aprotic solvent. Thus, the higher activation barrier for decarboxylation in the protic solvents results from the diminution in numbers and

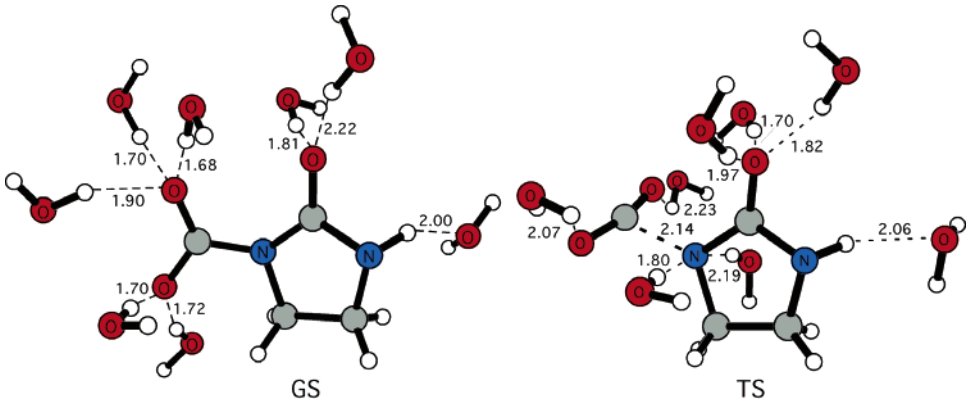

FIGURE 4. Snapshots of the reactant **2** (GS) and the transition state (TS) for the decarboxylation in water with hydrogen-bonded water molecules retained. O−H and N−H distances in Å.

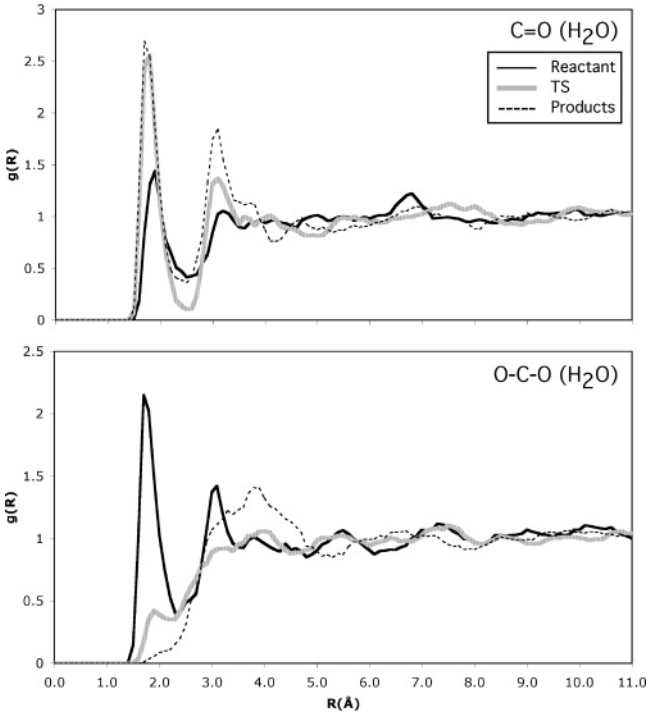

FIGURE 5. Computed ureido C═O···H─(H_2O) (top) and carboxylate O─C─O···H─(H_2O) (bottom) radial distribution functions for the reactant **2**, the TS, and the products.

strength for hydrogen bonds in progressing to the more charge-delocalized TS. Owing to the analogous stabilization of the product anion by hydrogen bonding, it is also worth noting that the activation barrier for the reverse reaction, carboxylation of imidazolidin-2-onyl anion, is also significantly higher in water than in acetonitrile (Figure 2). Hydrogen bonding pulls down both ends of the free-energy profiles. Thus, reduction in hydrogen-bond stabilization of reactant anions by both carboxylase and decarboxylase enzymes would be kinetically advantageous.

A related observation from the crystal structures of avidin─biotin and streptavidin─biotin complexes,[23] as well as from molecular dynamic simulations,[24] is that the ureido oxygen of biotin accepts three hydrogen bonds, for example, from the side chains of Asn23, Ser27, and Tyr43 for streptavidin. This is consistent with the images in Figure 4, however, the coordination of water can be better quantified through computed radial distribution functions (rdfs). These are shown in Figure 5 for the interactions of the ureido and carboxylate oxygens of the biotin model **2**, the TS, and the products with hydrogens of water. Hydrogen bonds are reflected in the first peaks, which extend to O···H distances of about 2.5 Å. For the reactant **2**, it is apparent that the hydrogen bonding is much greater for the carboxylate oxygens than for the ureido oxygen. Then the pattern inverts for the TS and product as the charge is transferred from the carboxylate group. Integration of the first peaks in the rdfs gives averages of 2.6 and 6.0 hydrogen bonds with water molecules for the ureido and carboxylate oxygens in **2**. These numbers become 3.0 and 2.8 for the TS and 3.6 and 0.7 for the product. The results are particularly interesting for catalyst design as they do indicate that positioning of three hydrogen-bond donating or Lewis acidic entities for interaction with the ureido oxygen in the TS is optimal, as in Figure 4 (TS). Two hydrogen-bond donors for the ureido N in the TS also appear desirable, and an obvious benefit would derive from shielding the carboxylate group in the reactant from its full complement of hydrogen-bond donors.

Mixed Solvents. Rahil et al. also measured the rates for decarboxylation of **2** in methanol─water and acetonitrile─water mixtures, and, as expected, the rates increase with decreasing water content.[9b] This has been pursued here computationally to further test the robustness of the methodology and to gain insight into the variations in TS structure with solvent composition and of differential solvation in the mixed media, that is, solvent segregation to optimize solvation of a solute. To our knowledge, this is the first report of FEP results for an organic reaction in mixed solvents. Free-energy profiles were computed in a similar fashion as for the pure solvents with R_{NC} ranging from 1.40 to

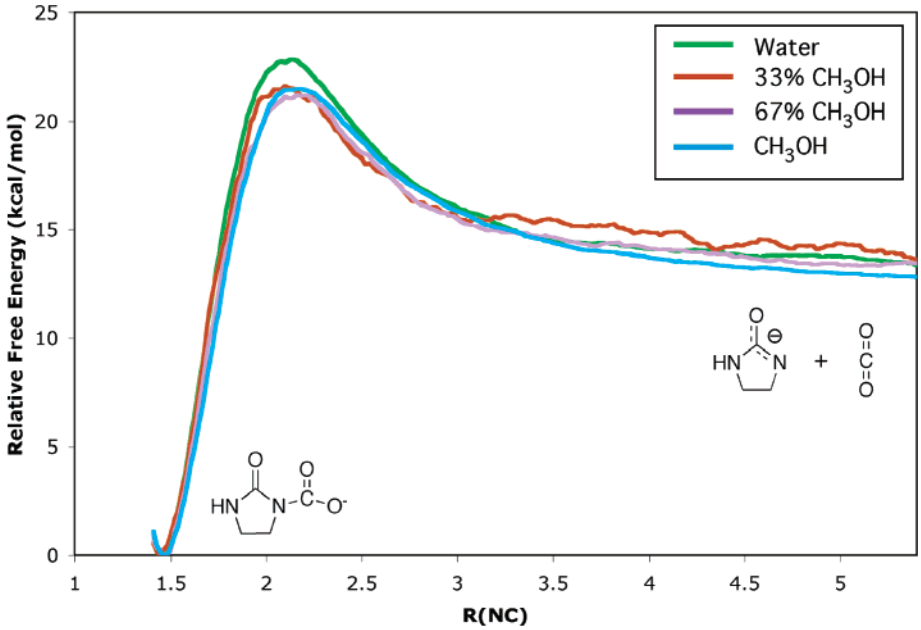

FIGURE 6. Computed free-energy profiles in pure water, 33 and 67% methanol mixtures, and pure methanol for the decarboxylation of **2**.

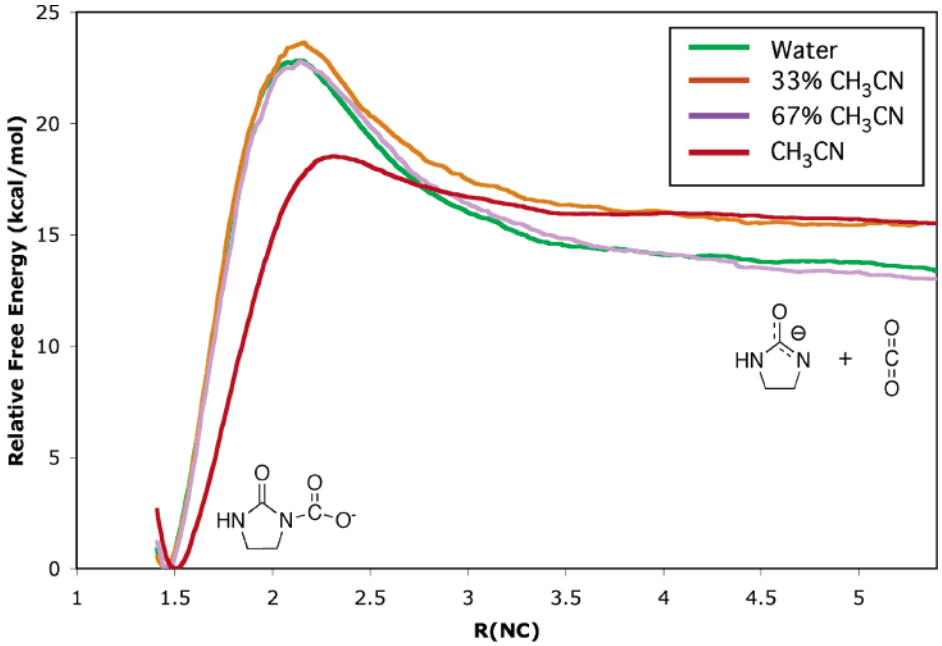

FIGURE 7. Computed free-energy profiles in pure water, 33 and 67% acetonitrile mixtures, and pure acetonitrile for the decarboxylation of **2**.

TABLE 3. Free Energies of Activation and Reaction (kcal/mol) for the Decarboxylation of 2 in Methanol−Water Mixtures

CH_3OH (%)	$\Delta G^{\ddagger}$ (calcd)	$\Delta G^{\ddagger}$ (exptl)[a]	ΔG_{rxn} (calcd)
0	22.8	23.2	13.4
33	21.6	22.8	13.6
67	21.2	22.1	13.5
100	21.5	20.9	12.8

[a] Reference 9b.

TABLE 4. Free Energies of Activation and Reaction (kcal/mol) for the Decarboxylation of 2 in Acetonitrile−Water Mixtures

CH_3CN (%)	$\Delta G^{\ddagger}$ (calcd)	$\Delta G^{\ddagger}$ (exptl)[a]	ΔG_{rxn} (calcd)
0	22.8	23.2	13.4
33	23.6	22.7	15.5
67	22.8	22.0	13.0
100	18.5	19.5	15.5

[a] Reference 9b.

TABLE 5. Computed R_{NC} Distances (Å) for the TS for Decarboxylation of 2 in Aqueous Solvent Mixtures at 25 °C and 1 atm

	0%	33%	67%	100%
CH_3OH	2.14	2.10	2.16	2.18
CH_3CN	2.14	2.16	2.14	2.32

5.40 Å in increments of 0.01 Å; however, the MC sampling was increased to 10 million configurations of equilibration and 5 million configurations of averaging to allow full solvent relaxation. Experimentally, 33.3 and 66.6% solvent mixtures were studied.[9] Here, the mixed systems were comprised of a total of 395 molecules in a tetragonal periodic cell. Thus, given the experimental densities at 25 °C and 1 atm, for example, a 33.3% v/v acetonitrile/water mixture contains 59 acetonitrile and 341 water molecules, while a 66.6% acetonitrile/water mixture contains 164 acetonitrile and 236 water molecules. The BOSS program automatically sets up the mixed systems by

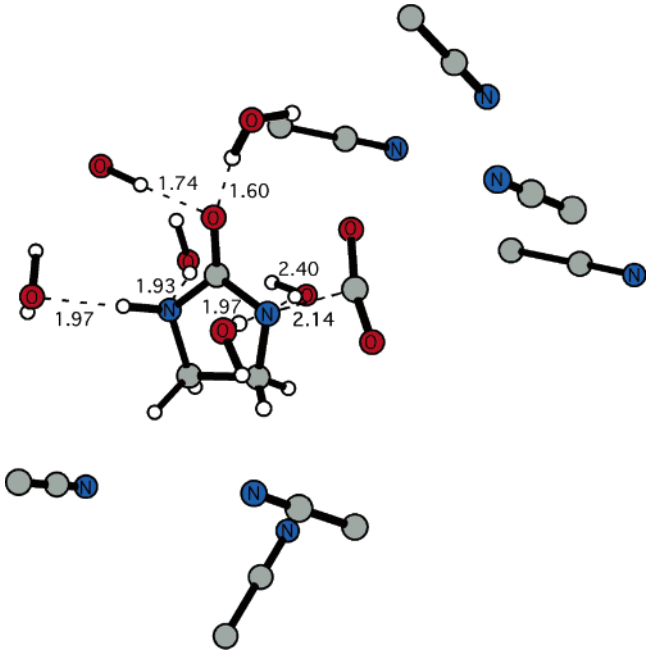

FIGURE 8. Snapshot of a transition structure for the decarboxylation of **2** in 67% aqueous acetonitrile. Nearby water and acetonitrile molecules are retained; distances in Å.

starting from a stored box of the pure solvent with larger molecular volume and randomly replacing the correct number of solvent molecules with molecules from the other component.[14]

The computed free-energy profiles as a function of solvent composition are shown in Figures 6 and 7. The expected pattern is found with decreasing barrier heights as the percentage of

(23) (a) Weber, P. C.; Ohlendorf, D. H.; Wendoloski, J. J.; Salemme, F. R. *Science* **1989**, *243*, 85−88. (b) Weber, P. C.; Wendoloski, J. J.; Pantoliano, M. W.; Salemme, F. R. *J. Am. Chem. Soc.* **1992**, *114*, 3197−3200.

(24) Miyamoto, S.; Kollman, P. A. *Proteins* **1993**, *16*, 226−245.

water decreases; the quantitative accord with the experimental free energies of activation remains excellent (Tables 3 and 4). The geometrical results are particularly interesting, as is apparent in Figures 6 and 7 and summarized in Table 5. The only free-energy profile that shows a significant shift in the location of the TS is for pure acetonitrile. The origin of the longer R_{NC} distances in acetonitrile and the gas phase were discussed above. However, as long as water is present, the TS occurs at an R_{NC} distance of 2.14 ± 0.02 Å. This suggests that the important hydrogen-bonding interactions with water are maintained at the TS for the 33 and 67% solvent compositions. Display of configurations supports this view, as illustrated for the 67% acetonitrile solution in Figure 8. Five or six water molecules cluster near the ureido group and donate hydrogen bonds to the formally negatively charged ureido N and O. This is similar to the situation in pure water, for example, Figure 4 (TS). The presumably weaker hydrogen bonds with the emerging CO_2 are sacrificed. Simultaneously, the acetonitrile molecules are seen to cluster on the less-polar side of the TS in Figure 8.

Conclusions

QM/MM/FEP simulations have been carried out for decarboxylation of the biotin model **2** in both pure and mixed solvents with good success in reproducing the experimentally observed free energies of activation. Analysis of solute−solvent structures and energetics confirms the expectation that the slower reaction rates in protic versus dipolar aprotic solvents stem from loss of hydrogen bonding in going from the carboxylate anion **2** to the more charge-delocalized TS. For analogous reasons, the barrier for the reverse carboxylation process was also found to be greater in the protic solvents. Furthermore, the structure of the TS is significantly affected by the reaction medium; it occurs at a 0.2-Å shorter C−N separation in protic solvents than in acetonitrile to enhance hydrogen bonding at the TS. Additional characterization of the hydrogen bonding provided insights for decarboxylase catalysts, namely, it is desirable to have three hydrogen-bond donating groups positioned to interact with the ureido oxygen along with two hydrogen-bond donors positioned to interact with the ureido nitrogen of the breaking C−N bond. Destabilization of the reactant through reduction of hydrogen bonding with its carboxylate group would also be clearly beneficial. As modeled here for acetonitrile as solvent, transfer from water to a less-polar environment is in this spirit. Other potentially productive possibilities are known including manipulation of the protonation state of the cofactor or substrate in view of the far greater reactivity of protonated biotin or **1** than their conjugate bases and Lewis-acid complexation with the ureido oxygen.[1,5−9]

Acknowledgment. Gratitude is expressed to the National Science Foundation (CHE-0446920), the National Institutes of Health (GM032136), and the Alabama Supercomputer Center for support of this research. Discussions with Prof. Ronald Kluger were also appreciated.

Supporting Information Available: Additional energy pair distributions for the decarboxylation of **2** in pure methanol and solvent mixtures and coordinates for the transition structures in Figures 4 and 8 are provided. This material is available free of charge via the Internet at http://pubs.acs.org.

JO060533B